



Gentile, Lorenzo and Giugliano, Dario and Cestino, Enrico and Frulla, Giacomo and Minisci, Edmondo (2018) Optimisation based analysis of the effect of particle spatial distribution on the elastic behaviour of PRMMC. In: 6th European Conference on Computational Mechanics and 7th European Conference on Computational Fluid Dynamics 2018, 2018-06-11 - 2018-06-15. ,

This version is available at <https://strathprints.strath.ac.uk/65673/>

Strathprints is designed to allow users to access the research output of the University of Strathclyde. Unless otherwise explicitly stated on the manuscript, Copyright © and Moral Rights for the papers on this site are retained by the individual authors and/or other copyright owners. Please check the manuscript for details of any other licences that may have been applied. You may not engage in further distribution of the material for any profitmaking activities or any commercial gain. You may freely distribute both the url (<https://strathprints.strath.ac.uk/>) and the content of this paper for research or private study, educational, or not-for-profit purposes without prior permission or charge.

Any correspondence concerning this service should be sent to the Strathprints administrator: strathprints@strath.ac.uk

OPTIMISATION BASED ANALYSIS OF THE EFFECT OF PARTICLE SPATIAL DISTRIBUTION ON THE ELASTIC BEHAVIOUR OF PRMMC

Gentile Lorenzo^{1*}, Giugliano Dario^{2*}, Cestino Enrico³, Frulla Giacomo³,
Minisci Edmondo²

¹ TH Köln
Steinmüllerallee 6, 51643, Gummersbach
lorenzo.gentile@th-koeln.de

² University of Strathclyde
Montrose Street 75, G1 1XJ, Glasgow
dario.giugliano@strath.ac.uk

³ Politecnico di Torino
Corso Duca degli Abruzzi 24, 10129, Torino

* The authors contributed equally.

Key words: Optimisation, Genetic algorithms, SMBO, Computational homogenisation, MMCs

Abstract. A study of particle reinforced metal matrix composite (PRMMCs) by means of periodic multi-particle unit cells is presented. The inhomogeneous particle spatial distribution, as well as the effect of matrix/particles interface, strongly influences the heterogeneous material behaviour. The effect of both particle spatial distribution and particle size effect on the uniaxial elastic response of PRMMCs is addressed. The uniaxial tensile loading on cubicshaped cells with a different number of spherical particles (up to 50) and different fraction volumes (up to 25%) is studied by using Abaqus FEA [?], Matlab Global Optimisation Toolbox and the R Sequential Parameter Optimisation Toolbox SPOT [?]. Three different optimisation processes are used i.e. high-fidelity optimisation, low-fidelity optimisation and surrogate assisted optimisation that takes into account the uncertainty in particle spatial distribution. Accurate finite element analyses (FEA) on different representative volume elements (RVEs) have been conducted by means of Abaqus-optimizer coupling and computational homogenization. Numerical upper bound (UB) and lower bound (LB) of the homogenized uniaxial Young's modulus E_x , based on high fidelity model based optimisation techniques (HFMBBO), are reported. A memetic algorithm with adaptive parameter control optimisation process based on a model derived by sensitivities analysis is proposed. The results are compared to the ones using a surrogate assisted optimisation with Kriging. In the latter case, uncertainty in particle spatial distribution has been considered in regards to the current limited control in manufacturing techniques. The results show that the analytical upper bounds' models

overestimate predictions especially in configurations with a low number of particles per RVE. The results of the different optimisation processes have been compared and, the importance of the critical parameters on Ex has been addressed.

1 INTRODUCTION

Metal Matrix Composites (MMCs) are strong candidates for the design of components into the applications where the property profile of conventional materials either does not reach the increased standard of specific demands or is the solution of the problem. The aim of using MMCs is in reducing the weight and improving the thermomechanical properties of components and performance at elevated temperatures while maintaining the maximum ductility [?]. Among the aforementioned MMCs, particulate reinforced composites can have costs comparable to unreinforced metals with significantly better hardness and somewhat better stiffness and strength. The response of PRMMCs on the basis of computational simulations aimed at searching the optimal design has been under the attention of designer and researchers over the last two decades [?, ?, ?, ?, ?]. The most important analytical models for investigating the thermomechanical behaviour of PRMMCs comprises variational methods, mean field approaches based on Eshelby's inclusion [?], and statistically based descriptions [?]. In search of different modelling strategy, a large number of studies of MMCs have been reported in which unit cells are employed. Microfield approaches based on finite element method (FEM) are capable of providing the complex stress and strain fields generated in periodic composite's phases upon deformation. However, realistic unit cell models for describing the elastoplastic response of PRMMCs are computationally expensive and therefore, most of such studies have been limited to planar or highly regular three-dimensional RVEs [?] as well as modifications thereof [?]. For PRMMCs, three-dimensional unit cells appear to be the latest development in modelling the monotonic and the cyclic behaviour of PRMMCs with different shapes of the reinforcement [?, ?, ?, ?, ?]. Various studies have demonstrated the capabilities of this method to predict with high fidelity the effective properties of particle-reinforced composites subjected to elastic [?, ?] and elasto-plastic deformation [?, ?, ?]. Based on the same modelling technique, the effect of damage initiation and evolution has been addressed as reported in [?, ?, ?].

The present work concentrates on investigating the particle spatial distribution and particle size effect on the homogenized elastic behaviour of particle reinforced metal matrix composites by means of optimisation techniques. Among them, the memetic optimisation process used for this work has been employed due to the robustness guaranteed by stochastic search. Moreover, multilevel approaches by means of local optimisation, monotonic basin hopping and adaptive control parameter pledged efficient convergence rate even in high dimensional optimisation. We propose an approach that tackles the problem of optimizing the characteristics of PRMMCs subject to uniaxial load taking also into account the uncertain particle's placement. The optimisation problem is split into a bilevel problem i.e. the upper-level optimisation aims to find the particle dis-

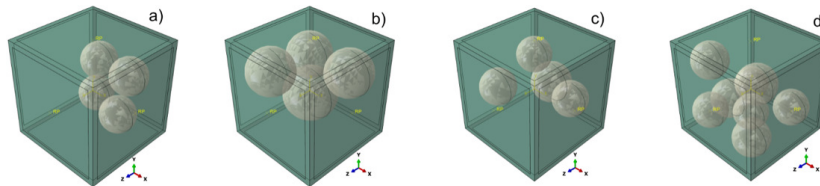


Figure 1: Idealized three-dimensional periodic unit cells: a) $V_f=10\%$ and $N_{part} =4$ UB, b) $V_f =20\%$ and $N_{part} =4$ UB, c) $V_f=10\%$ and $N_{part} =4$ LB, d) $V_f=20\%$ and $N_{part} =8$ UB.

tribution parameters which maximize the PRMMC uniaxial Young's Modulus and the lower-level problem that attempts to create a particle placement that reflects the specifications of an upper-level candidate solution due to potentially infeasible distributions. We employed a Surrogate Model Based Optimisation (SMBO) approach that combines Kriging, Sequential Parameter Optimisation and a Genetic Algorithm.

2 Problem description

Idealized three-dimensional periodic cells, which consist of elastic reinforcing spherical particles embedded in an elastoplastic matrix (Fig.1), are considered to optimize the homogenized Young's modulus along the x direction, hereinafter referred to as Ex . Genetic algorithm, bilevel SMBO and computational homogenization [?] have been employed for the aforementioned purpose. The former two have been coupled with Abaqus FEA to investigate the effect of particle spatial distribution aimed at optimizing Ex for a given fraction volume and number of particles. The latter is used to average the local behaviour of the composites' constituents within the RVE in order to compute Ex .

The study starts with a high-fidelity model based optimisation (HFMBO). This is employed to evaluate the inclusion's arrangement that maximizes (Upper Bound) and minimize (Lower Bound) Ex . All geometries are meshed by Abaqus C3D10 tetrahedral elements and a typical model is comprised of about 60000 elements. Constituent material properties were chosen to correspond to elastic SiC particles perfectly bonded to an Aluminium 6061-T6 matrix that follows the data reported in Table ?? [?, ?]. Periodic boundary conditions (PBC) are applied to the unit cells faces as reported in [?]. The generation of the multi-inclusion unit cells starts by choosing the number of particles, hereinafter referred to as N_{part} , (from 1 to 8) and the particles fraction volume, hereinafter referred to as V_f , (10%, 15%, 20%) so that the particle size can be selected. Next, upon applying PBC, the elastic behaviour is investigated by means of uniaxial tensile load. Afterwards, a sensitivity analysis has been performed and, in light of the results, a low fidelity based model optimisation (LFMBO) is conducted over a wider range of number of particles per RVE (from 1 to 20) and V_f (from 10% to 25%). Finally, an additional SMBO is used proposed to extend the research on arrays characterized by a higher number of particles per RVE (1-50) and $V_f=10\%$. Adopting this approach the uncertainty on particle distribution due to manufactory process is considered.

Table 1: Material properties: Uniaxial stiffness, Poisson’s number, Yield stress, Ultimate tensile stress.

	E [GPa]	ϵ	σ_{p0} [GPa]	UTS [GPa]
Al6061-T6	68.9	0.3	276	310
SiC	380	0.19	-	1500

2.1 HFMBO and LFMBO methods

A generic optimisation problem can be formulated as described in Eq. ??:

$$Optimisation \left\{ \begin{array}{l} \text{Maximize } f(x) \\ x_i \in [x_i^{lb}, x_i^{ub}], i = 1, \dots, n \\ g_j \leq 0, j, \dots, J \\ h_{k(x)} = 0, k = 1, \dots, K \end{array} \right. , \quad (1)$$

where g_j represent the inequality constraints, h_k the equality constraints and x_i^{ub} and x_i^{lb} are the highest and lowest values that the n variables (each describing one particle position along one axis) x_i can assume (box constraints). In this research two different constraints are imposed:

$$\left\{ \begin{array}{l} x_x^i, x_y^i, x_z^i \geq l_b + r + \Delta, i = 1, \dots, N_{part} \\ x_x^i, x_y^i, x_z^i \leq u_b - r - \Delta, i = 1, \dots, N_{part} \\ C_{ij} = \Delta - \sqrt{(x_x^i - x_x^j)^2 + (x_y^i - x_y^j)^2 + (x_z^i - x_z^j)^2} \leq 0, \\ i, j = 1, \dots, N_{part}, j \neq i \end{array} \right. , \quad (2)$$

Particles fully embedded in the matrix imposed trough box constraints and inclusions separation imposed through inequality constraints: where l_b are the particles centre coordinates along the x, y and z axes, $l_b = 0, u_b = 10$ represent the coordinates of the matrix bounds, r is the particles radius and $\Delta = 0.2$ is the minimum distance between matrix and particles surface.

2.2 High-Fidelity Model Based Optimisation

HFBO is based on the integrated approach which relies upon the coupling between Matlab Global Optimisation Toolbox, Python [?] and Abaqus FEA. In HFMBO $f(x)$ in Eq.?? consists in Ex. The black-box nature of the objective function, the consequent infeasibility of providing additional information such as the objective function gradient and the ambition of finding the global optimum, led to the development of a genetic algorithm (GA) based optimisation process. A Latin hypercube design of experiments that generates only feasible candidates, employing a local dummy optimisation, has been adopted to generate the first population of candidates. The objective function Ex is evaluated by coupling different software modules e.g. Matlab Objective function Code and a set of Python scripts for Abaqus FEA which is comprised of RVE generator, PBC

adaptive code, pre-processing code and homogenization code. Whenever a candidate is feasible i.e. both the box constraints and nonlinear constraints are satisfied (Eq.??), the objective function works as wrapper function to interface GA to the RVE Generator code. The latter generates the FE models according to the optimisation variables values while the pre-processing code automatically assigning materials properties, generates the mesh, applies the concentrated force on the dummy node, runs the PBC code and submits the simulations. The PBC Adaptive Code is used to guarantee that the simulations results generated would represent a macro structure consisting of periodically-repeated cells. Upon defining three node groups on the boundary faces i.e. inner face nodes, inner edge nodes and corner nodes, we impose a set of equations as reported in [?] which will be applied between the relative node pairs.

Upon completing a FE simulation, from the Abaqus output database (ODB), the homogenization code calculates the uniaxial Young's modulus, E_x , by computing the ratio between the homogenized stress $\tilde{\sigma}_x$ and the homogenized strain $\tilde{\epsilon}$ along the x direction [?] as follows:

$$E_x = \frac{\tilde{\sigma}_x}{\tilde{\epsilon}_x} = \frac{\sum_{i=1}^{N_{ip}} \sigma_i V_i}{V_{tot}} / \frac{\sum_{i=1}^{N_{ip}} \epsilon_i V_i}{V_{tot}}, \quad (3)$$

where N_{ip} is the number of integration points, V_i is the volume of each integration point, V_{tot} is the total array volume and σ_i and ϵ_i are the stress and strain measured at each integration point. Afterwards, E_x is returned to the optimisation process as objective function value. In case of infeasible candidates, the process involving Abaqus is skipped and E_x is assigned making use of a penalty function as follows:

$$E_x = E_m - \sum_i C_{ns} \quad (4)$$

where E_m is the matrix Young's modulus and C_{ns} are all the ns constraints not satisfied. When the "Evaluation" step is completed, the candidates are ranked and selected generating the mating pool on which the classical GA operators will generate the new candidate's population. However, to reduce the number of infeasible candidates, on the infeasible children resulting from the operators, an additional local dummy optimisation is performed. If the stopping criteria are not satisfied, the optimisation loop is restarted from the proposed new population.

2.3 Low-Fidelity Model Based Optimisation

Afterwards the HFMBBO, a sensitivity analysis has been conducted in order to identify the variables correlation that mostly affects E_x . The results pointed out that two parameters strongly influence E_x :

- Particles overlap in the plane normal to the applied stress defined as:

$$OverlapArea = \sum_k \binom{N_{part}}{1} 2\pi r_i \arctan(y_k, x_k) + r_j^2 atan(y_k, d(i, j) - x_k) - d(i, j)y_k \quad (5)$$

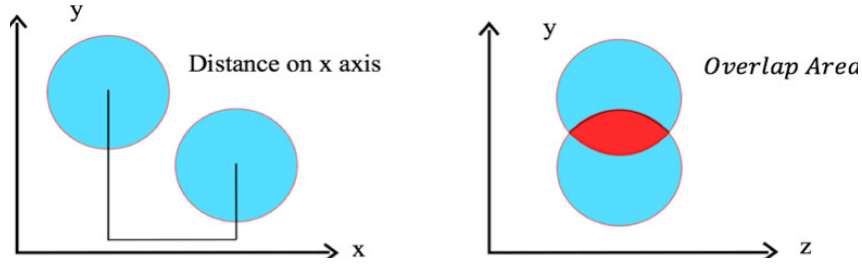


Figure 2: Overlap Area and distance on x axis for the RVE with 2 particles.

where $x_k = \frac{(r_i^2 - r_j^2 + d(i,j)^2)}{sd(i,j)}$ and $y_k = \sqrt{(r_i^2 - r_k^2)}$

- Distance between particles in the direction of the applied stress defied as:

$$\sum_k \binom{N_{part}}{1} |x_i - x_k| \quad (6)$$

where $x_k = \frac{(r_i^2 - r_j^2 + d(i,j)^2)}{s*d(i,j)}$ and $y_k = \sqrt{(r_i^2 - r_k^2)}$ Unlike the parameter Overlap Area, that has a strong influence on E_x independently to its value, the parameter representing the distance on the x axis influences the configurations with low E_x value (Fig.2). As a consequence, if the assumption that the search space is restricted to a region in which $E_x \propto OverlapArea$ holds, the optimisation of *OverlapArea* and E_x have a one-to-one correspondence. Hence, the optimisation process has been modified considering the Overlap Area as the objective function. This means that, referring Eq.??, in LFMBO $f(x) = OverlapArea$. Switching the objective function from the FEA result to an analytical parameter entails a considerable reduction of computational cost (from about 20s to about 1 ms) that made advantageous the use of a more effective optimisation process. In LFMBO a memetic algorithm, in which the local exploitation has been performed through a Monotonic Basin Hopping (MBH) algorithm [?] has been adopted. Moreover, looking for a more performing exploration phase, adaptive selection settings and adaptive stopping criteria control parameters have been used [?]. The optimisation process starts with a Latin Hypercube design of experiment and the most promising candidates are selected to constitute the first-generation population. Then, for each candidate the analytical value (objective function) defined in Eq.??, is calculated and, taking into account the constraints violation, a fitness value is assigned. Next, a ranking of the candidates is performed and, in line of current parameter controls, the most promising ones are selected and used by the GA operators to generate the next-generation population. Afterwards, with a probability of 5%, an MBH based local optimisation is performed starting from the actual best candidate and the population is drugged by the resultant solution that replaces the one used as MBH starting point. In order to have non-static control parameters, the mutation and crossover fraction are determined by the number of generations gone by the one with the best fitness value of 95% of the actual one. When the mutation and crossover fraction assume respectively the values of 0.8 and 0.2, the stopping criteria's count starts. The stopping criterion counts the number of past generations from the

last control parameters change and it is satisfied if the count arrives at 100. However, an additional stopping criterion that limits the number of generation to 10E4 is imposed. The optimisation process continues restarting the loop from the proposed next population until the stopping criteria are satisfied. Once the optimisation is reputed terminated, to evaluate the Ex value, a FEA is performed by means of the "Evaluation" process used in the HFMBO.

3 Surrogate Model Based Optimisation with uncertainty

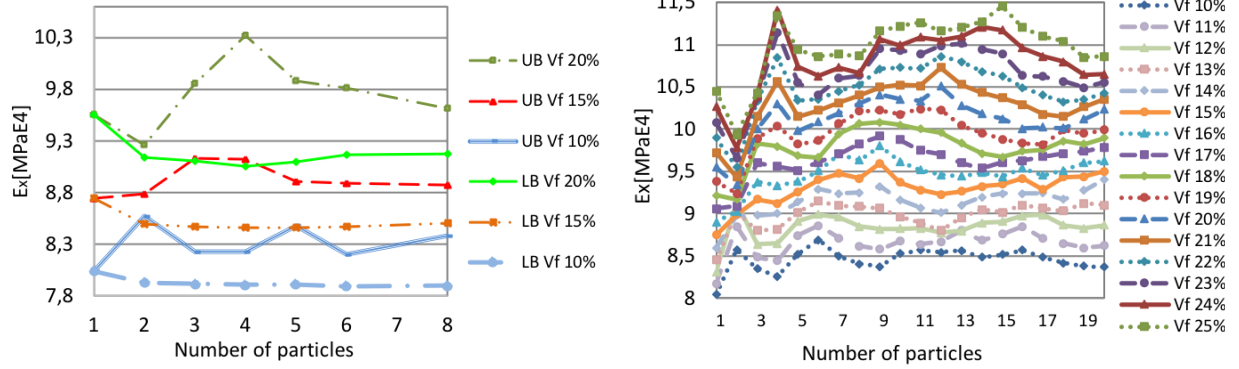
A PRMMCs optimisation that takes into account particle placement uncertainty has been developed and applied on the RVEs with Vf=10%. Particles are not deterministically placed but are assumed to be normally distributed along the three axes [?]. The number of particles (2-50) in the RVEs and the characteristics of the normal distribution are to be optimized. The problem has been formulated as a bilevel, nonlinear, constrained optimisation problem. The upper-level specifies the spatial distribution characteristics, specified by the number of particles and standard deviations in each dimension that maximizes Ex. The lower-level consists of determining a feasible spatial distribution holding the properties specified by the upper-level candidate solutions. To solve the upper-level optimisation problem, we require a method that accounts for the stochastic and expensive nature of the problem. Hence, we used the Sequential Parameter Optimisation Toolbox (SPOT), which is an implementation of the SPO in the programming language R. Among the surrogate models available in SPOT, we used Kriging. The main assumption of Kriging is that the data follows a multi-variate Gaussian distribution, where errors are spatially correlated. More details about Kriging model implementation adopted can be found in [?]. The problem formulation, that coincides with the upper-level optimisation, is the follows:

$$\begin{aligned} \text{Find max } & f(Npart, \sigma_x, \sigma_y, \sigma_z) = E_x & (7) \\ \text{subject to } & \begin{cases} 2 < Npart < 50 \\ 0.7 < \sigma_x, \sigma_y, \sigma_z < 3 \end{cases} , & (8) \end{aligned}$$

where $Npart$ is the number of particles per RVE, $\sigma_x, \sigma_y, \sigma_z$ are respectively the standard deviations of the particle placements along the x, y, and z axes. A L-BFGS-B algorithm has been employed to perform the optimisation on the metamodel.

The goal of the lower-level optimisation is to specify the exact positions of all particles, that respects the statistical properties specified by an upper-level candidate solution. Therefore, the objective function to be minimized is defined as the deviation between actual sample statistics and the desired distribution. Formally, the lower-level optimisation problem can be defined as:

$$\begin{aligned} \text{Find min } & g(x_x^i, x_y^i, x_z^i, i = 1, \dots, Npart) = \left| std(x_x^1, \dots, x_x^{Npart}) - \sigma_x \right| + \\ & \left| std(x_y^1, \dots, x_y^{Npart}) - \sigma_y \right| + \left| std(x_z^1, \dots, x_z^{Npart}) - \sigma_z \right| , & (9) \end{aligned}$$



(a) Comparison between upper and lower bounds of E_x related to HFMBO. (b) Results related to LFMBO's UB for a wider range of N_{part} and V_f .

Figure 3: Deterministic optimisations results.

subject to the constraints illustrated in Eq. ???. The interest in a globally optimal solution, the lack of preliminary information about the objective function features and the necessity of a robust optimizer lead us to adopt an evolutionary algorithm for this task. Particularly, the Genetic Algorithm (GA) available in the R package GA [?] because of its robustness and ease of use has been employed.

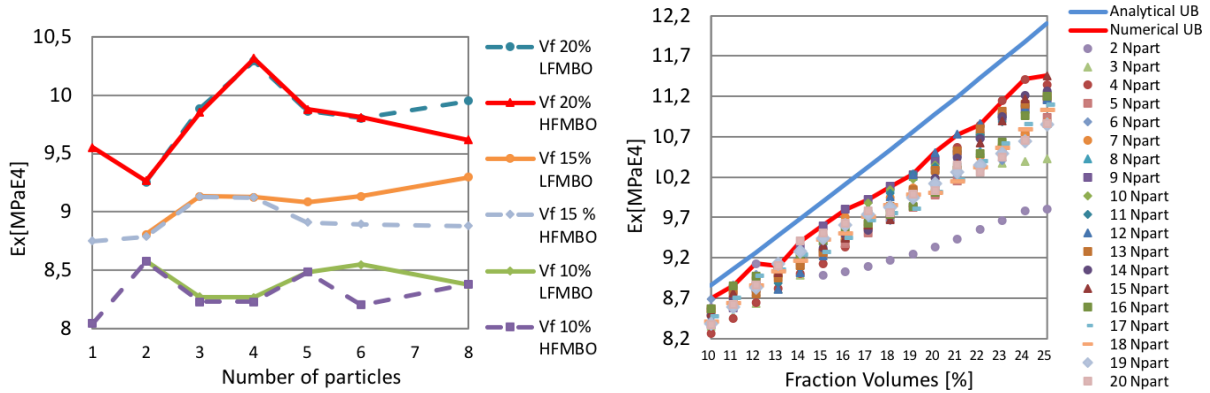
The feasibility of all the upper-level proposed candidate solution is not guaranteed. Therefore, the lower-level optimisation may result into particle placements that follow a distribution that is different from the desired one. To overcome this problem, SPO was modified to allow for updating proposed candidate solutions *after* they were evaluated.

3.1 High-fidelity Model Based Optimisation results

The upper and lower bounds of E_x at different number of particles per RVE (1,2,3,4,5,6,8) and different fraction volumes of the reinforcement (10%, 15%, 20%) have been evaluated. The results are shown in Fig.3-a. The obtained results highlight that the reinforcement fraction volume, the number of particles and the particles' arrangement influence the value of E_x . Indeed, taking into account the RVEs $N_{part}=4$ with $V_f=10\%$ (Fig.1-a) and $N_{part}=4$ with $V_f=20\%$ (Fig.1-b), both related to the UB, it is possible to explain the increase of E_x because of the augment of V_f while the RVEs $N_{part}=4$ with $V_f=10\%$ (Figure 1-a) related to the UB, and $N_{part}=4$ with $V_f=10\%$ (Fig.1-c) related to the LB, clarify the variation of E_x with the particles' arrangement. In addition, by comparing the RVEs $N_{part}=4$ with $V_f=20\%$ (Fig.1-b) and $N_{part}=8$ with $V_f=20\%$ (Fig.1-d), the variation of E_x with the number of particles is addressed.

3.2 Low-fidelity Model Based Optimisation Results

LFMBO has been used to optimize a wider range of RVEs with different V_f (10% to 25%) and N_{part} (1 to 20) and the results are shown in Fig.3-b. In order to validate the results of E_x computed by LFMBO, a comparison with the HFMBO has been made and the accuracy of the LFMBO's prediction has been confirmed by the results that differ



(a) Comparison between HFMBO and LFMBO (b) Comparison between the LFMBO's results and upper and lower bounds predicted by Hashin and Shtrikman method.

Figure 4: Results comparison.

of less than 5% (Fig.4-a). A further comparison has been made between the analytical upper bound prediction of Hashin and Shtrikman method [?], where the particle spatial distribution is not considered and the values of Ex computed by LFMBO. It is evident from Fig.4-b that the analytical prediction overestimates the Young's modulus for all the Vf and Npart investigated and the higher the fraction volume the higher the percentage error between the analytical and numerical results (Fig.4-b).

3.3 SMBO with uncertainty results

The results obtained by the upper-level optimisation agree with the ones obtained with the HFMBO and by LFMBO. The optimum design, found after 226 real function evaluation, is $x_{opt} = (2.96, 1.61, 0.8, 5)$. The reader can see that in the optimum configuration, particles will tend to assume a rather narrow distribution with respect to the x-plane and spread in the x-axis. This means that the arrangement tends to align the particles increasing the Overlap Area, supporting the theory proposed in the LFMBO. With this optimal configuration, a value of $Ex = 8.34E4 MPa$ has been determined. One can see that this value is below the optimum find adopting the LFMBO. This result is not surprising because taking in account the uncertainty and hence having a limited control on the particle positions results less performing materials. However, adopting this method, we were able to examine configurations with a high number of particles per RVE.

4 Conclusions

A study on the elastic behaviour of particle reinforced metal matrix composites (PRMMCs) has been presented in this article. The effect of the particle's arrangement, number of particles and particle volume fraction on the upper and lower bounds of the uniaxial Young's modulus Ex has been investigated by means of 3D multi-particle unit cells and optimisation techniques. A first study has been conducted with a high-fidelity model

based optimisation (HFMBBO) framework which is based on the coupling between Matlab Global Optimisation Toolbox, Abaqus and Python . The importance of two parameters i.e. Overlap Area and distance on x axis, which influence in a different way the value of E_x has been addressed through a sensitivity analysis of the HFMBBO's results. By exploring the effect of these two parameters, a more effective low-fidelity model based optimisation (LFMBBO) , characterized by adaptive control parameter, stopping criteria and exploration through MBH based optimisation, has been proposed and the upper bound of E_x has been extended to a wider range of particles per RVE (from 1 to 20) and V_f (from 10% to 25%). The findings clearly indicate that the influence of the particle fraction volume V_f is predominant i.e. the higher the V_f the higher the E_x , instead the influence of N_{part} and the particle distribution has a complex behaviour their interaction. A proposed method expresses this interaction trough an intuitive analytical parameter, the Overlap Area. Also, the extended results show that a strong influence of particle spatial distribution on E_x is seen in configuration with a low N_{part} per RVE i.e. from 1 to 5 for all the V_f investigated, while for a higher N_{part} the value of E_x is more stable. The results obtained, have been compared with the theoretical upper bound predicted by the analytical model of Hashin and Shtrikman, and the comparison has identified that the analytical upper bound overestimates the results especially for high fraction volumes. A sophisticated approach that relies on surrogate models have been employed to extend the research on a wider range of configurations (V_f 10%, N_{part} 2-50). Employing this method has been optimized the particle spatial distribution considering the current level of control in manufactory processes. The use of the R package SPOT adopting Kriging as metamodel allowed to obtain a near-optimum configuration with a limited computation effort. This research has shown an effective methodology based on optimisation techniques and FEA simulations which can be extended to a wider range of applications in the composites field.

Acknowledgements

This work is partially funded by the European Commission's H2020 programme, through the UTOPIAE Marie Curie Innovative Training Network, H2020-MSCA-ITN-2016, Grant Agreement number 722734.

REFERENCES

- [1] Karlsson Hibbitt. *ABAQUS: User's Manual*. Hibbitt, Karlsson and Sorensen, Incorporated, 1997.
- [2] Thomas Bartz-Beielstein. *Experimental Research in Evolutionary Computation—The New Experimentalism*. Natural Computing Series. Berlin, Heidelberg, New York: Springer.
- [3] Karl U Kainer. *Metal matrix composites: custom-made materials for automotive and aerospace engineering*. John Wiley and Sons, 2006.
- [4] Helmut J Bhm and Wensheng Han. Comparisons between three-dimensional and two-dimensional multi-particle unit cell models for particle reinforced metal matrix

- composites. *Modelling and Simulation in Materials Science and Engineering*, 9(2):47, 2001.
- [5] Helmut J Bhm, Wensheng Han, and Anton Eckschlager. *Multi-inclusion unit cell studies of reinforcement stresses and particle failure in discontinuously reinforced ductile matrix composites*. na, 2004.
- [6] Javier Segurado, J LLorca, and C Gonzlez. On the accuracy of mean-field approaches to simulate the plastic deformation of composites. *Scripta Materialia*, 46(7):525–529, 2002.
- [7] J LLorca and J Segurado. Three-dimensional multiparticle cell simulations of deformation and damage in sphere-reinforced composites. *Materials Science and Engineering: A*, 365(1):267–274, 2004.
- [8] O Pierard, C Gonzalez, J Segurado, J LLorca, and Issam Doghri. Micromechanics of elasto-plastic materials reinforced with ellipsoidal inclusions. *International Journal of Solids and Structures*, 44(21):6945–6962, 2007.
- [9] John D Eshelby. The determination of the elastic field of an ellipsoidal inclusion, and related problems. In *Proceedings of the Royal Society of London A: Mathematical, Physical and Engineering Sciences*, volume 241, pages 376–396. The Royal Society.
- [10] Valerie A Buryachenko. The overall elastoplastic behavior of multiphase materials with isotropic components. *Acta Mechanica*, 119(1):93–117, 1996.
- [11] Craig L Hom and Robert M McMeeking. Plastic flow in ductile materials containing a cubic array of rigid spheres. *International journal of plasticity*, 7(4):255–274, 1991.
- [12] DF Watt, XQ Xu, and DJ Lloyd. Effects of particle morphology and spacing on the strain fields in a plastically deforming matrix. *Acta materialia*, 44(2):789–799, 1996.
- [13] HF Chen and Alan RS Ponter. On the behaviour of a particulate metal matrix composite subjected to cyclic temperature and constant stress. *Computational materials science*, 34(4):425–441, 2005.
- [14] W Ogierman and G Kokot. Particle shape influence on elastic-plastic behavior of particle-reinforced composites. *Archives of Material Science and Engineering*, 67(2):70–76, 2014.
- [15] Leon Mishnaevsky. Numerical mesomechanical experiments: Analysis of the effect of microstructures of materials on the deformation and damage resistance. *Computational Mesomechanics of Composites: Numerical analysis of the effect of microstructures of composites on their strength and damage resistance*, pages 129–150.
- [16] C Guillemer-Neel, V Bobet, and M Clavel. Cyclic deformation behaviour and baushinger effect in ductile cast iron. *Materials Science and Engineering: A*, 272(2):431–442, 1999.
- [17] Wensheng Han, Anton Eckschlager, and Helmut J Böhm. The effects of three-dimensional multi-particle arrangements on the mechanical behavior and damage initiation of particle-reinforced mmcs. *Composites science and technology*, 61(11):1581–1590, 2001.
- [18] Zvi Hashin and Shmuel Shtrikman. A variational approach to the theory of the elastic behaviour of multiphase materials. *Journal of the Mechanics and Physics of Solids*, 11(2):127–140, 1963.

- [19] J Segurado and J Llorca. A numerical approximation to the elastic properties of sphere-reinforced composites. *Journal of the Mechanics and Physics of Solids*, 50(10):2107–2121, 2002.
- [20] Dario Giugliano, Daniele Barbera, and Haofeng Chen. Effect of fiber cross section geometry on cyclic plastic behavior of continuous fiber reinforced aluminum matrix composites. *European Journal of Mechanics-A/Solids*, 61:35–46, 2017.
- [21] Dario Giugliano and Haofeng Chen. Micromechanical modeling on cyclic plastic behavior of unidirectional fiber reinforced aluminum matrix composites. *European Journal of Mechanics - A/Solids*, 59:155–164, 2016.
- [22] S Ghosh and S Moorthy. Particle fracture simulation in non-uniform microstructures of metalmatrix composites. *Acta Materialia*, 46(3):965–982, 1998.
- [23] Jinuk Kim. Homogenization and uncertainty analysis for fiber reinforced composites. 2011.
- [24] Aluminum Association. *Aluminum standards and data*. Aluminum Association., 2000.
- [25] RD Carnahan. Elastic properties of silicon carbide. *Journal of the American Ceramic Society*, 51(4):223–224, 1968.
- [26] Guido Van Rossum. Python programming language. In *USENIX Annual Technical Conference*, volume 41, page 36.
- [27] Ghayath Al Kassem and Dieter Weichert. Micromechanical material models for polymer composites through advanced numerical simulation techniques. *PAMM*, 9(1):413–414, 2009.
- [28] David J Wales and Jonathan PK Doye. Global optimisation by basin-hopping and the lowest energy structures of lennard-jones clusters containing up to 110 atoms. *The Journal of Physical Chemistry A*, 101(28):5111–5116, 1997.
- [29] Àgoston E Eiben, Robert Hinterding, and Zbigniew Michalewicz. Parameter control in evolutionary algorithms. *IEEE Transactions on evolutionary computation*, 3(2):124–141, 1999.
- [30] Lorenzo Gentile, Martin Zaefferer, Dario Giugliano, Haofeng Chen and Thomas Bartz-Beielstein. Surrogate assisted optimisation of particle reinforced metal matrix composites. *Proceedings of the Genetic and Evolutionary Computation Conference 2018*, 8, 2018
- [31] Alexander Forrester, Andy Keane et Al. *Engineering design via surrogate modelling: a practical guide*. John Wiley & Sons.
- [32] Luca Scrucca. GA: A Package for Genetic Algorithms in R. *Journal of Statistical Software*, 53(4):1–37, 2013.